ELSEVIER

Biophysical Chemistry 51 (1994) 9–19

Biophysical Chemistry

Site-specific counterion binding: Application of the standard Poisson–Boltzmann cell model to ionic polysaccharides of the plant cell wall

M. Voué, C. Gillet

Laboratoire de Biotechnologie Théorique, Facultés Universitaires de Namur, 5000 Namur, Belgium

(Received 6 October 1993; accepted in revised form 4 January 1994)

Abstract

A numerical method is presented for analysing the effects of the competitive processes of dissociation and complexation that occur at the level of the functional groups of charged polysaccharides during ion exchange experiments carried out on plant cell walls. The interactions between the exchange sites and the mobile ions are handled by the standard Poisson–Boltzmann cell model. The dissociation and the complexation are described by mass-action laws. Uncomplexed counterions are involved in the formation of a cylindrical double layer. This latter type of interaction determines the dissociation degree of the polyion. A least-squares algorithm is used to evaluate the complexation constants of the counterions from experimental data. The need of introduction of the complexation constant of the divalent counterions has been clarified by a comparison between theoretical titration curves calculated with and without specific site binding. The fraction of complexed sites does not agree with that predicted from Oosawa's theory of the condensation. The accumulation coefficients, calculated from the optimised theoretical titration curves, clearly demonstrate the competition between the protonation and the complexation processes at the level of the pectic acids of the wall.

Key words: Plant cell wall; Polyelectrolyte; Poisson–Boltzmann cell model; Counterion binding; Polygalacturonic acid; Nitella flexilis

1. Introduction

The Poisson–Boltzmann cell model (PBCM) has been intensively used to describe the thermodynamic properties of polyions in solution [1–8]. In this paper, we use this model to analyse the importance of the electrostatic binding of the counterions to specific sites of the constitutive pectic acids of the plant cell wall. The pectic acids are polymers of the α-(1,4)-linked galacturonic acid residues (Fig. 1) eventually interspaced with neutral sugars, mainly α-(1,2)-linked rhamnosyl residues. They play an important role as natural ionic exchangers. In *Nitella flexilis* (L.) Ag., a giant freshwater alga of the Characeae family, the sequential chemical analysis shows that the internodal cell wall is composed of about 31% of pectins, the remaining polysaccharides being uncharged (37% of cellulose and 25% of hemicellulose) [9–11]. There are also 7% of cell wall proteins which may significantly contribute to the total charge of the wall at alkaline pH only.

SSDI 0301-4622(94)00003-3

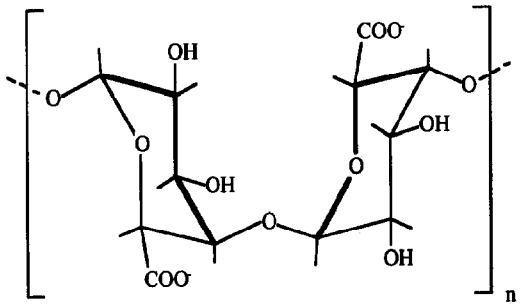

Fig. 1. Repeating structure of pectic acids based on α-(1,4)-linked galacturonic acid residues.

As the experiments described in this study were carried out in the 1.0 to 6.0 pH range, it seems reasonable to consider that the pectins are the only charged macromolecules of the wall. More than 93% of the pectins in *Nitella* are unmethylated [12,13], a result confirmed by ^{13}C NMR experiments [14]. In solution, the distance separating two successive charges in a homo-polygalacturonic acid chain is about 4.35 Å. It can be continuously varied by either protonation and complexation of the exchange sites of the polymer or by association of the polyelectrolyte chains into dimers and multimers as the result of a divalent cations (Ca^{2+}, Cu^{2+} or Mn^{2+}) bridging process as proposed for the alginates in the 'egg-box model' (Fig. 2) [15,16]. In the plant cell wall, the variations of the mean charge separation and its influence on the subsequent conformational modifications of the constitutive pectic acids does not seem to be so clear for two major reasons: the validity of the egg-box model when applied to the wall has never been undoubtedly verified and the polysaccharide chains of the wall are subject to mechanical constraints difficult to modelise which considerably modify the swelling and the gelling properties with respect to those observed in solution.

In the frame of the PBCM, we describe the ion exchange reaction of the plant cell wall with the ions of its environment as an equilibrium reaction between the dissociation of the exchange sites and their possible complexation by the counterions. Combining the dissociation–complexation equilibrium with the PBCM yields the surface complex model [17], a generalisation of the models of ionizable double layers encountered in bio-

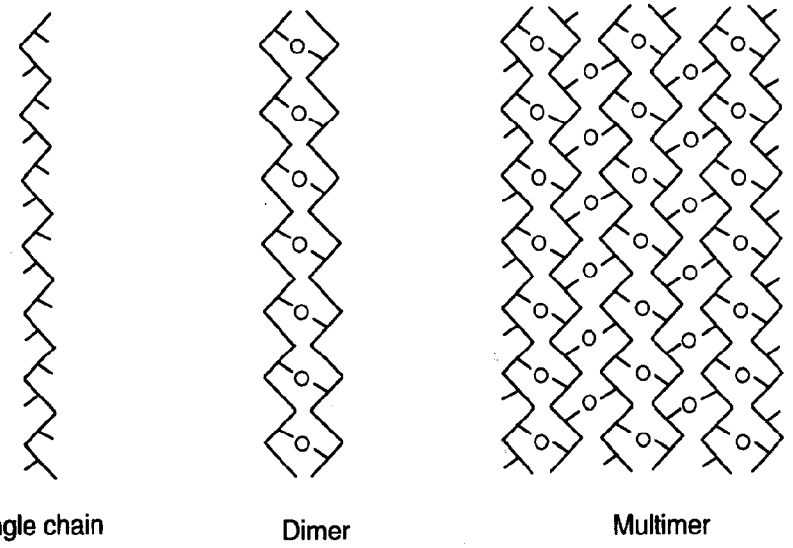

Fig. 2. The 'egg-box' model. The association of homopolygalacturonic sequences (broken lines) in dimers and multimers is made by a divalent cations (O) bridging process.

logical membranes [18–20]. In this work, the 'complex' term is used to describe the purely electrostatic complexes (i.e. those in which the cation remains separated from the ligand by its hydration layer) but also the covalent ones. Within the framework of the surface complex model, the cations interact with the exchange sites according to two different modes. In the first interaction type, the metallic cations combine with deprotonated sites to form either inner- or outer-sphere complexes, regarding to a possible partial dehydration accompanying the complexation. The second interaction mode is purely electrostatic. It assumes the formation of flat or cylindrical double layers around the exchange sites, according to the chosen geometry. In this approach, only the deprotonated and uncomplexed sites contribute to the formation of the electrical double layer. As quoted by Nilsson and Piculell [7], this approach of the site binding process is entirely phenomenological in the sense that nothing needs to be assumed about the structure of the exchange site itself. Nevertheless, the study of the dissociation–complexation equilibrium in the plant wall remains an important step towards the understanding of the relation of the small mobile ions with the fixed negative charges of the pectic matrix.

In this paper, H^+-Mn^{2+} ion exchanges were carried on the plant cell wall of *Nitella flexilis* (L.) Ag. and the results were compared with the predictions of the surface complex model under the assumption that the electrostatic properties of the wall are mainly due to the homopolygalacturonic sequences.

2. Theory and computations

2.1. Ion exchange reaction

The competitive processes of protonation and of complexation of the exchange sites of the polyion are described by mass action laws that contribute to the global ion-exchange reaction. This reaction does not depend on the geometry chosen to describe the polyion. Each ion-exchange reaction taking place at the level of the exchange site X^- of the cell wall between one z-valent metallic cation M^{z+} and z protons may be written as

$$zHX_{(s)} + M^{z+}_{(aq)} \rightleftharpoons MX_{z(s)} + zH^+_{(aq)}, \tag{1}$$

where the (s) and (aq) subscripts are respectively used to describe the solid and aqueous phases. The exchange thermodynamic constant associated to this reaction is

$$K_{ex} = \frac{(MX_z)_{(s)}(H^+)^z_{(aq)}}{(HX)^z_{(s)}(M^{z+})_{(aq)}}, \tag{2}$$

where parentheses are used for activities. This constant K_{ex} is the product of two constants associated to partial reactions

$$K_{ex} = K_d^z K_{MX_z}, \tag{3}$$

with K_d the constant of the dissociation reaction of the exchange site leading to the release of protons in the vicinity of the site

$$HX_{(s)} \rightleftharpoons X^-_{(s)} + H^+_{(aq)}, \tag{4}$$

and K_{MX_z} the stability constant associated to the complexation reaction of the metallic cations at the exchange site level

$$zX^-_{(s)} + M^{z+}_{(aq)} \rightleftharpoons MX_{z(s)} \tag{5}$$

In the solid phase, the dissociation degree α is defined by the ratio of the dissociated sites to the total amount of sites expressed on a water content basis

$$\alpha = \frac{(X^-)}{(X_{tot})}. \tag{6}$$

β_i is the occupation fraction of the ionic species i, i.e. the fraction of the total amount of sites complexed with the type i cations (the i subscript runs over all the ionic species of the aqueous phase). Explicitly,

$$\beta_i = \frac{(MX_z)}{(X_{tot})}. \tag{7}$$

The dissociated fraction α and the occupation fractions β_i are related by

$$\alpha = 1 - \sum_i z_i \beta_i. \tag{8}$$

In a mixture of 1–1 and 2–1 electrolytes with a common coion and M^{2+} and N^{+} counterions, the occupation fractions β_i are expressed as functions of the dissociation constant K_d, of the stability constants of the complexes K_{NX} and K_{MX_2} and of the dissociation degree α. For the protons, the N^{+} and the M^{2+} counterions, the occupation fractions β_i are respectively given by

$$\beta_H = \frac{\alpha(H^+)}{K_d}, \tag{9a}$$

$$\beta_1 = \alpha K_{NX}(N^+), \tag{9b}$$

$$\beta_2 = \alpha^2 K_{MX_2}(M^{2+})(X_{tot}). \tag{9c}$$

For greater readability, the subscripts (s) and (aq) have been omitted in Eqs. (6)–(9). Provided a set of values for K_d, K_{NX} and K_{MX_2} is known, these relations can be combined with (8) to yield a quadratic equation in α, whose solution is

$$\alpha = -\frac{1+(H^+)K_d^{-1}+K_{NX}(N^+)}{4K_{MX_2}(M^{2+})(X_{tot})} + \left\{\left[\left[1+(H^+)K_d^{-1}+K_{NX}(N^+)\right]^2 + 8K_{MX_2}(M^{2+})(X_{tot})\right]^{1/2}\right\} \times \left\{4K_{MX_2}(M^{2+})(X_{tot})\right\}^{-1}. \tag{10}$$

As the stability and dissociation constants have been defined as intrinsic and not as apparent thermodynamic constants, the concentrations involved in the mass-action laws are the concentrations in the immediate vicinity of the exchange sites [21]. The electric field created by the progressive ionisation induces an accumulation of

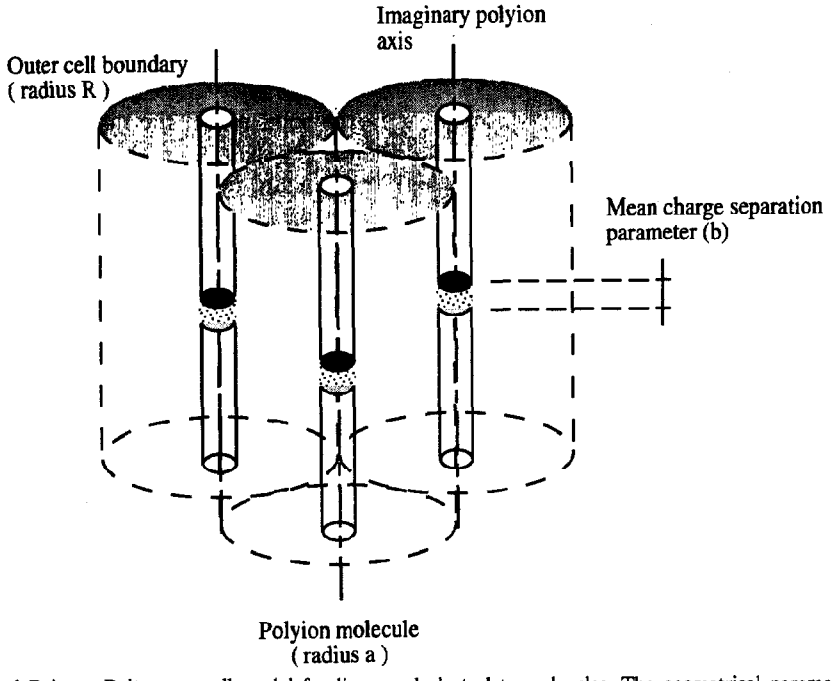

Fig. 3. Standard Poisson–Boltzmann cell model for linear polyelectrolyte molecules. The geometrical parameters used in the numerical solution of the Poisson–Boltzmann equation are the polyion radius (a), the outer cell boundary (R) and the mean charge separation parameter (b).

counterions in the vicinity of the functional groups. Therefore, the values of the concentrations of the mobile ions may highly differ from the one in the bulk solution. Such values are to be computed from a theoretical model in a given geometry. A classical approach is provided by the Poisson–Boltzmann cell model.

2.2. Poisson–Boltzmann cell model

The PBCM has been extensively used to describe the ionic atmosphere surrounding locally linear polyelectrolyte molecules in solution. The solution is divided in cylindrical cells whose radius R is calculated from the polyion concentration. Each cell contains one polyion that occupies the central position and is aligned along the longitudinal axis of the cylinder. The polyion molecule has a non-zero finite radius a which represents the shortest approach distance for the mobile small ions (Fig. 3). The solvent is represented by a dielectric continuum with relative permittivity ϵ_r. The surface charge density σ of a polyion carrying monovalent functional groups is related to the cell parameters by

$$\sigma = \frac{e}{2\pi ab}, \tag{11}$$

where b is the mean charge spacing along the axis of the cylindrical cell, e is the elementary charge. The concentration profiles in the standard cell are given by the numerical solution of the Poisson–Boltzmann equation. This equation forms the basis of the classical theory of the electrical double layer. It treats the mobile ions of the solution as point-like charges ignoring their mutual correlations and its numerical solution semi-quantitatively describes the ionic distributions around the polyion but has been shown thermodynamically consistent [22]. For the cylindrical system, it reads

$$\frac{1}{r}\frac{\mathrm{d}}{\mathrm{d}r}\left(r\frac{\mathrm{d}\phi}{\mathrm{d}r}\right) = -\frac{1}{4\pi\epsilon_0\epsilon_r}\sum_i \rho_{i0}\exp\left(-\frac{z_i e\phi}{kT}\right), \tag{12}$$

where ϕ is the mean electrostatic potential, r is the distance from the axis of the cell and ρ_{i0} is the charge concentration of ionic species i in the bulk solution. The appropriate boundary conditions, given by the Gauss law, are

$$\left(\frac{\partial\phi}{\partial r}\right)_{r=a} = -\frac{\sigma}{\epsilon_0\epsilon_r} \quad \text{and} \quad \left(\frac{\partial\phi}{\partial r}\right)_{r=R} = 0. \tag{13}$$

The Poisson–Boltzmann equation is solved with a so-called 'shooting method' [23,24], yielding a mean electrostatic potential profile across the cell.

2.3. Numerical procedures

In pectic acids, the protonation and the complexation of the exchange sites by the metallic counterions are competitive processes that both contribute to a neutralisation of the surface charge density σ. The dissociation increases it while the complexation has the opposite effect. The balance between the purely electrostatic interactions and the binding of the counterions is treated self-consistently at the Poisson–Boltzmann level. Each step of the iterative process requires the knowledge of the ionic concentrations in the vicinity of the polyion and therefore a numerical solution of the Poisson–Boltzmann equation. The process is initiated by assuming that the pectic acids are completely dissociated. Once the mean electrostatic potential profile is known, the ionic distributions and their volume averages can readily be calculated. Eqs (10), (12) and (13) are repeatedly solved [25] until the Poisson–Boltzmann equation and the mass-action laws are satisfied. Once the numerical algorithm has converged, the occupation fractions β_i are computed from (9) to evaluate the proportion of complexed cations.

3. Materials and experimental methods

The plants used were specimens of *Nitella flexilis* (L.) Ag. grown in pond water in laboratory tanks. Internodal cells 4 cm long were excised from the axis and their ends cut with a razor blade. Two stainless steel wires were introduced in the so-formed cylinder and separated from

each other to obtain a flat wall rectangle. These pieces of cell wall were washed in ethanol and diethylether to remove the contaminants of the cytoplasm. The walls were then equilibrated in polyethylene vials containing 20 ml of 5 mM $MnCl_2$. This solution was renewed every hour during 8 h. This experimental procedure ensures the total replacement of the ionic content of the wall, especially of Ca^{2+} ions. Afterwards, the pre-treated walls in Mn^{2+} form were equilibrated in 0.05 mM, 5 mM or 25 mM $MnCl_2$ solutions at pH varying from 1.0 to 6.0, the solutions being renewed every hour. After 8 h treatment, the equilibrated walls were dried by blotting between two Whatman No. 3 filter papers, weighed on an electrobalance and their ionic content extracted overnight in 2 ml of a 1 M HCl solution. The extract was analysed by flame atomic absorption spectrophotometry (Philips PU 9200 X). From a physiological point of view, the use of a 2–1 electrolyte at these concentrations inhibit the degradation of the cell wall that takes place when its ionic environment contains only alkaline ions [26,27].

4. Results and discussion

4.1. Model parameters

In the following study, we suppose that the electrostatic properties of the plant cell wall are mainly determined by the homopolygalacturonic sequences of the pectin molecules. The wall is therefore assimilated to an homogeneous solution of pectic acid although it has been shown to be chemically as well as physically highly heterogeneous [28,29]. This drastic hypothesis is partially relaxed by two factors: (a) the presence of the neutral sugars which influences the degree of swelling of the wall, is implicitly taken into account in the evaluation of the outer radius of the Poisson–Boltzmann cell and (b) the fact that the electrical charges are not uniformly distributed throughout the whole space, as stated in the hypothesis of the classical Donnan model [30], but are aligned along the axis of the standard cells.

As previously quoted, the cell radius is determined by the monomer concentration. The mean water content of the cell walls, which is a measure of the free volume accessible to the mobile ions, has been found to be 3.5 liter per kg of dry weight while the concentration of the polygalacturonic acid monomer equals 0.385 M. From these values, the calculated outer radius of the cell is 18.5 Å, whereas the closest approach distance between the polyion molecules and the mobile ions is 5.0 Å [31]. The volume fraction of the pectins is therefore equal to 0.27. As the mean distance separating two charges in a homopolygalacturonic chain is 4.35 Å, these parameters yield a surface charge density σ equal to -0.117 C/m^2. In our calculations, the dissociation pK of the PGA acid molecules is assumed to be equal to 3.36, the pK value of the monomer.

4.2. Complexation of the manganese ions in the Nitella wall

4.2.1. Comparison of the model predictions with the experimental results

Due to the removal of the water from the wall phase during the drying of the samples (cf. Section 3), the experimental Mn^{2+} contents are the sum of the amount of complexed cations and of the excess of Mn^{2+} that electrostatically screens the ionised pectic acids. This excess of the ion i is given by the integral of the concentration profile c_i across the free volume V of standard cell and corrected for the concentration at the outer limit of the cell $c_{i,R}$

$$\Gamma_i = \int_V (c_i - c_{i,R})\, dV. \tag{16}$$

If the standard cell only contains one monomer of the polyion chain, the summation of all these excess Γ_i (weighed by the unsigned valence) on all the ionic species is nothing else than the dissociation degree α of the polyion. For these reasons, we propose to compare the experimentally determined fractions X_i to the theoretical ones $X_{i,\mathrm{th}}$ calculated by

$$X_{i,\mathrm{th}} = \beta_i + |z_i|\,\Gamma_i, \tag{17}$$

where the subscript i runs over all the counterions species. In this relation, the first term corresponds to the complexed fraction while the second one represents the double layer contribution. Practically, the complexation constants are evaluated by fitting the theoretical fractions $X_{i,th}$ given by (17) to the experimental ones X_i; each step of the least-squares algorithm requiring numerous iterative solutions of the Poisson–Boltzmann equation.

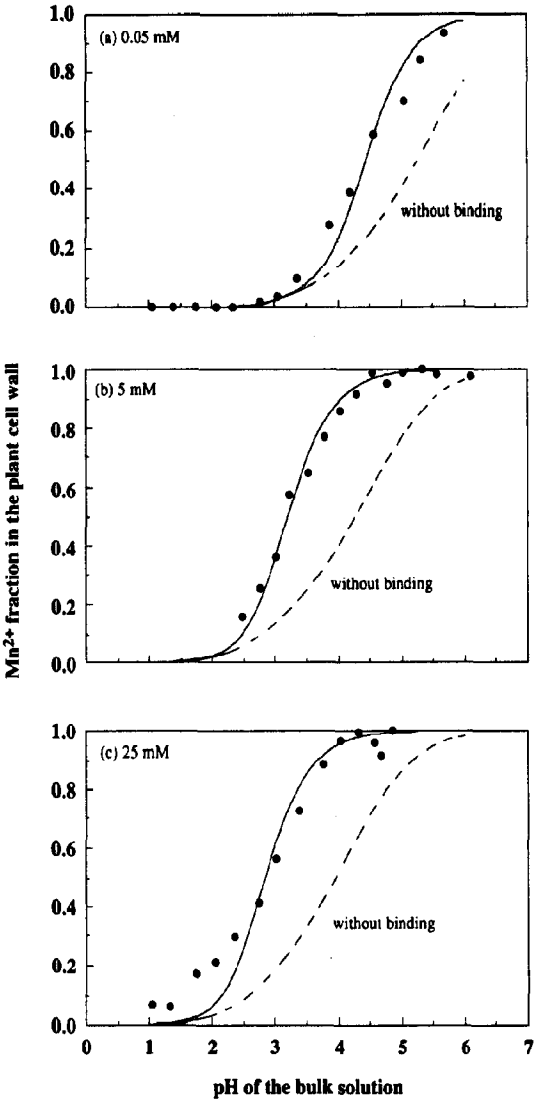

Fig. 4. Influence of the pH of the bulk solution on the fraction of fixed Mn^{2+} counterions in the *Nitella flexilis* cell wall. The $MnCl_2$ concentration in the bulk solution is (a) 50 μM, (b) 5 mM and (c) 25 mM. The solid lines correspond to the theoretical fractions calculated after optimisation of the complexation constant of the Mn^{2+} counterions. These values are summarised in Table 1. The dashed lines represent the fraction of Mn^{2+} counterions accumulated in the vicinity of the exchange sites of the wall if the specific site binding is neglected.

4.2.2. Dissociation profile of the Nitella polygalacturonic acids in $MnCl_2$ environment

In Figs. 4a–4c, the ion exchanges between the protons and the Mn^{2+} ions in the *Nitella* wall are presented in the form of titration curves. The concentrations of $MnCl_2$ in the treatment solution are 0.05 mM, 5 mM and 25 mM, respectively. Fig. 4 shows the fraction of sites occupied by the Mn^{2+} ions as a function of the pH which is varied from 1.0 to 6.0. The theoretical curves (plain lines) in Fig. 4 were calculated after the optimisation of the complexation constants. The optimised values of those constants are given in Table 1. The calculated curves including the site binding effects adequately reproduce the experimental data except at 25 mM, where a discrepancy is observed below pH 2.5. This effect may be explained by an overestimation of the cationic content in these experimental conditions due to the a contamination caused by the presence of large amounts of salt in the bulk solution. For each of the tested concentration, the theoretical fractions calculated in the absence of Mn^{2+} specific binding are also shown (dashed lines). This purely electrostatic model is unable to reproduce the experimental data. The discrepancy between both types of theoretical curves brings evidence for the specific binding of the Mn^{2+} counterions to the pectic acids. Therefore, it clarifies the need of introduction of the specific binding constants in the PBCM when applied to the plant cell wall.

The $MnCl_2$ concentration in the bulk solution does not influence the shape of the titration curve: although the salt concentrations varies on a wide range, each titration curve exhibits a typical sigmoid shape. The decrease of the salt concentration of the environment shifts the experimental data to the higher pH. From Fig. 4, it appears that the pH shift of the experimental data is approximately equals the square root of

Table 1
Influence of the bulk concentration on the logarithm of the complexation constant of the Mn^{2+} ions in the *Nitella* cell wall and on the thermodynamical constant of the H^+–Mn^{2+} exchange

	$MnCl_2$ concentration in the bulk solution (M)			Ref. [36] [a]
	50.0×10^{-6}	5.0×10^{-3}	25.0×10^{-3}	
$\log (K_{MnX_2})$	+2.40	+2.95	+2.98	
$\log (K_{ex})$	−4.32	−3.77	−3.74	−5.20

[a] Characteristics of the Mn^{2+}–H^+ ion exchange calculated according to the model of Van Cutsem and Gillet [36]. This model does not take into account the specific site binding of the divalent counterions.

the logarithm of the concentration ratio. This behaviour may be predicted from Eq. (2) provided that the characteristics of the ion exchanger do not depend on the salt concentration.

The increase of the $MnCl_2$ concentration in the bulk solution induces a slight modification of the binding and of the global exchange constants (Table 1). As the Mn^{2+} counterions have been shown to bind in a spacially sequential fashion [32], the influence of the salt concentration on the binding energy can be explained by cooperative effects due to the involvement of ordered conformations slightly depending of the counterion concentration. In these conditions, it is reasonable to suggest that an increase of the divalent cations concentration does not modify the basis of the ion exchange mechanism but induces minor modifications in the geometry of the exchange sites. The values that we found for the exchange constants are different from those of Deiana and co-workers [33] for the stability of the Mn^{2+}–polygalacturonate complexes in 10 mM NaCl solutions. They have evaluated the exchange constant by the graphical Bjerrüm method [34,35] and obtained $\log K_{ex} = -1.06$. They suggested the involvement of two carboxylate groups in the formation of outer-sphere complexes. The discrepancy between our results (Table 1) and the results of these authors may be explained by the fact that they used Na^+ counterions to adjust the

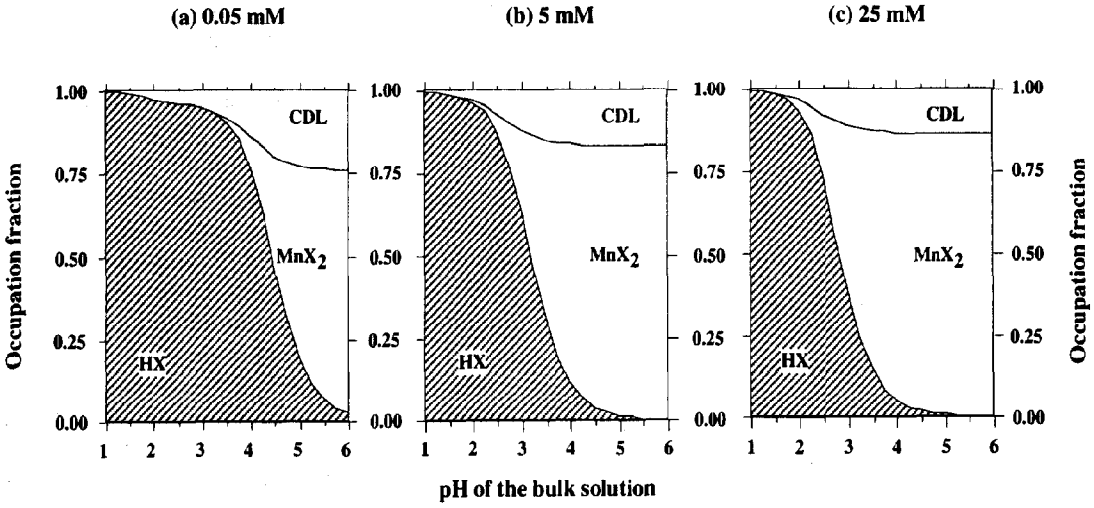

Fig. 5. Occupation diagrams of the exchange sites of the *Nitella* wall. The theoretical fractions are calculated with the optimised values of the complexation constant of the Mn^{2+} counterions. The $MnCl_2$ concentrations in the bulk solution are (a) 0.05 mM, (b) 5 mM and (c) 25 mM. Each kind of sites is respectively referred as HX (protonated), MnX_2 (complexed) and CDL (involved in the formation of a double layer). At a given pH, the vertical extent of the shaded areas gives the fraction of sites involved in any type of interaction.

ionic strength of their solutions. These monovalent counterions compete with the divalent ones and the binding constant are therefore reduced. Moreover, quantitative comparisons are made difficult by the polyion concentration (0.385 M) and by the mechanical constraints that exist in wall and limit the molecular motions. Our results are also different from those of Van Cutsem and Gillet [36] who evaluated the exchange constant in the plant cell wall without taking into account the possible site specific binding of the counterions. If we use their equation, corrected for the stoechiometry of our global exchange reaction (1), we obtain $\log K_{ex} = -5.2$.

Once the optimum parameters of the exchange are determined, the occupation fractions can readily be calculated. The results are presented in Fig. 5 in the form of an occupation diagram. According to the hypothesis of the surface complex model, the exchange site may exist under one of the three following forms: undissociated, complexed by a divalent cation or involved in a double layer. Each kind of site is respectively referred as HX, MnX_2 and CDL; the latter corresponding to the dissociation degree α. The diagram shows, for each type of exchange site, the influence of the pH of the solution on its occupation level. At a given pH, the vertical extent of the shaded areas gives the fraction of sites involved in any type of interaction. The decrease of the salt concentration induces a delayed ionisation of the sites as shown by the importance of the protonated fraction (HX type sites) at 0.05 mM. Most of the ionised sites are complexed by the Mn^{2+} ions whereas the cylindrical double layer remains localised to less than 25% of the exchange sites, even at full ionisation. Inasmuch as our basic assumptions concerning the site-specific counterions binding are correct, this would mean that the Donnan behaviour of the plant cell wall, as proposed by Dainty and Hope [37], is questionable in the sense that not all the deprotonated exchange sites of the wall are involved in the Donnan model.

Although the thermodynamic state of the bound Mn^{2+} ions in the PBCM is different from that of the condensed counterions which, in the condensation (CC) theory [38–40], are considered to be territorially bound and not site specific bound, it is interesting to compare the results originating from both theories. As the CC theory has only been successfully applied to the titration of polyelectrolytes with an excess of 1–1 salt, the results of Manning and co-workers [41,42] cannot be applied to analyse our experimental results carried out with mixtures of $MnCl_2$ and HCl. However, at full dissociation only, the fraction of sites involved in the formation of MnX_2 complexes can be roughly compared to the apparent degree of binding of the polyelectrolyte predicted by Oosawa's theory of the condensation [43]. The numerical solution of Eq. (67) in ref. [44] yields a value of 0.64 for the fraction of sites neutralised by counterion condensation is the absence of excess electrolyte. This value is lower than the fractions of complexed sites in the PBCM: 0.74 in 0.05 mM, 0.83 in 5 mM and 0.86 in 25 mM. These results clearly show that the CC theory is unable to describe quantitatively the interactions of the Mn^{2+} ions with the carboxylic exchange sites of the wall and that an additional specific site binding has to be introduced with that theory too.

As shown in Fig. 6, the mean electrostatic potential at the surface of the polygalacturonic acid (ϕ_s), reaches a stationary value at the highest pH. This value, calculated when the formation of MnX_2 complexes is taken into account, is considerably lower than that calculated in the absence of specific site binding (indicated by the black arrows in Fig. 6). Due the mass action law (5) that determines the formation of the complexes, the ϕ_s value is strongly influenced by the $MnCl_2$ concentration. From the comparison of Figs. 5 and 6, it also appears that the surface potential remains constant when the Mn^{2+} specific binding clearly dominates the protonation reaction i.e. above pH = 4.0 at 5.0 mM and 25.0 mM and above pH 5.0 at 0.05 mM.

Furthermore, for each ion species, the mean accumulation coefficient k, defined by the ratio of its mean concentration in the standard cell to its bulk concentration has been calculated. Results are presented in Table 2. As expected as a consequence of the electroselectivity of the PBCM, the protons accumulate less than the divalent cations do. At fixed salt concentration,

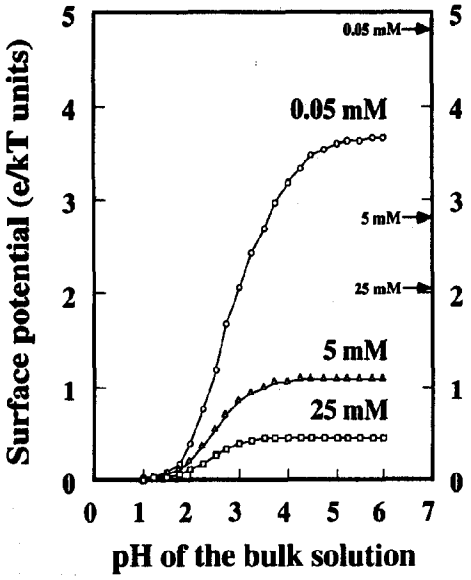

Fig. 6. Variation of the mean electrostatic potential (in e/kT units) at the surface of the polygalacturonic molecules as a function of the pH of the bulk solution. Limiting values calculated in the absence of specific binding are indicated by black arrows.

Table 2
Influence of the concentration and of the pH of the bulk solution on the accumulation coefficients of the protons (k_H), manganese ions (k_{Mn}) and chlorides (k_{Cl})

$MnCl_2$ conc. (M)	pH	Accumulation coefficients [a]			Γ_D (%) [b]
		k_H	k_{Mn}	k_{Cl} [c]	
5.0×10^{-5}	2.5	2.99	9.00	33.13	66.87
	3.5	12.34	153.20	8.05	91.95
	4.5	20.98	450.00	4.78	95.22
	5.5	23.07	548.00	4.39	95.61
5.0×10^{-3}	2.5	1.44	2.10	68.69	31.31
	3.5	1.96	3.92	50.78	49.22
	4.5	2.02	4.34	48.45	51.55
	5.5	2.06	4.36	48.30	51.70
25.0×10^{-3}	2.5	1.11	1.24	89.35	10.65
	3.5	1.19	1.43	83.66	16.34
	4.5	1.20	1.46	82.95	17.05
	5.5	1.20	1.46	83.00	17.00

[a] The accumulation coefficients k are defined as the ratio of the average concentration, calculated on the standard cell volume, to the bulk concentration.
[b] The Donnan exclusion ratio Γ_D describes the co-ions rejection (in %) and is defined by Eq. (18).
[c] The values of the accumulation coefficient of the Cl^- are multiplied by 100.

both k_H and k_{Mn} coefficients increase with the pH of the bulk solution. At fixed pH, a second effect is observed: when the Mn^{2+} bulk concentration increases, the values of those coefficients decrease. These two effects are explained by the two mechanisms that control the number of available exchange sites: the deprotonation of the sites which increases CDL fraction as the pH of the bulk solution increases (Fig. 5) and the binding of the Mn^{2+} cations which is more pronounced at high Mn^{2+} concentration, this mechanism contributing to the diminution of the CDL fraction. These effects are reversed in the case of the coions as it is shown by their accumulation coefficient k_{Cl}. The influence of the concentration of the bulk solution on the coions rejection is depicted by the values of the Donnan exclusion ratio Γ_D. This coefficient is defined by

$$\Gamma_D = \frac{C_{Cl} - \langle C_{Cl} \rangle}{C_{Cl}}, \tag{18}$$

where C_{Cl} is the coions concentration in the bulk solution and $\langle C_{Cl} \rangle$ is their mean concentration in the wall. A pH increase induces a deprotonation of the exchange sites according to Eq. (4) and a coions rejection characterised by a higher value of the Donnan rejection ratio Γ_D. A bulk concentration increase favours the replacement of the protons by the Mn^{2+} counterions, resulting in a lower value of Γ_D, because the average chloride concentration $\langle C_{Cl} \rangle$ nearly reaches the value of the bulk concentration. The Mn^{2+} increase in the bulk concentration acts at two different levels: it induces a better electrostatic screening of the exchange sites due to the electroselectivity of the divalent cations over the protons and, according to Eq. (5), it displaces the chemical equilibrium of the σ-regulating process towards the formation of MnX_2 complexes.

Concluding remarks. The strength of the above analysis lies in its ability to provide a unified description of the ion-exchange process in a solid heterogeneous polyelectrolyte phase, such as the plant cell wall, in terms of simple parameters: the complexation constants of the counterions. The surface complex model provides a more realistic description of the ion exchange processes

than the classical two-states Donnan model do: it allows the mobile ions to be continuously and non-uniformly distributed around the pectins molecules. The introduction of the complexation constant for the Mn^{2+} is assessed by the comparison between the theoretical titration curves calculated with and without specific binding. Our model is an alternative to the one proposed by Richter and co-workers [44,45]. Furthermore, it overcomes some experimental difficulties arising from the applicability of the counterion condensation theory. The study of the influence of the composition of the bulk solution and of the degradation of the polyion phase are currently in progress.

References

[1] R.M. Fuoss, A. Katchalsky and S. Lifson, Proc. Natl. Acad. Sci. 37 (1951) 579.
[2] T. Alfrey, P.W. Berg and H. Morawetz, J. Polym. Sci. 7 (1951) 543.
[3] R.A.J. Marcus, J. Chem. Phys. 23 (1955) 1057.
[4] L. Kotin and M. Nagasawa, J. Chem. Phys. 36 (1962) 873.
[5] D. Dolar and A. Peterlin, J. Chem. Phys. 50 (1969) 3011.
[6] B. Jönsson and H. Wennerström, J. Phys. Chem. 91 (1987) 338.
[7] S. Nilsson and L. Piculell, Macromolecules 24 (1991) 3804.
[8] M. Mandel, J. Phys. Chem. 96 (1992) 4934.
[9] L. Taiz, J.-P. Métraux and P.A. Richmond, Cytomorphogenesis in plants (Springer, Berlin, 1981).
[10] M.F. Alary-Bernard, M. Briens, M.G. Quillet and M. Goas, Phytochemistry 19 (1980) 1111.
[11] J.C. Morrison, L.C. Greve and P.A. Richmond, Planta 189 (1993) 321.
[12] H. Morikawa and M. Senda, Agric. Biol. Chem. 38 (1974) 1955.
[13] D.M.W. Anderson and N.J. King, J. Chem. Soc., (1961) 5333.
[14] P.L. Irwin, M.D. Sevilla and W. Chamulitrat, Biophys. J. 54 (1988) 337.
[15] G.T. Grant, E.R. Morris, D.A. Rees, P.J.C. Smith and D. Thom, FEBS Letters 32 (1973) 195.
[16] R. Kohn, Pure Appl. Chem. 42 (1975) 371.
[17] G. Sposito, The thermodynamics of soil solutions (Clarendon Press, Oxford, 1981).
[18] B.W. Ninham and V.A. Parsegian, J. Theoret. Biol. 31 (1971) 405.
[19] J. Barber, Biochim. Biophys. Acta 594 (1980) 253.
[20] J.N. Israelachvili, Intermolecular and surface forces with applications to colloidal and biological systems (Academic Press, New York, 1987).
[21] M. Guéron and G. Weisbuch, Biopolymers 19 (1980) 353.
[22] M. Fixman, J. Chem. Phys. 70 (1980) 4995.
[23] H. Mineur, Techniques de calcul numérique (Dunod, Paris, 1968).
[24] B. Carnahan, H.A. Luther and J.O. Wilkes, Applied numerical methods (Wiley, New York, 1969).
[25] J.F. Traub, Iterative methods for the solution of equations (Prentice-Hall, London, 1964).
[26] C. Gillet, P. Van Cutsem and M. Voué, J. Exp. Bot. 40 (1989) 129.
[27] C. Gillet, P. Cambier and F. Liners, Plant Physiol. 100 (1992) 846.
[28] K. Roberts, Curr. Opin. Cell Biol. 2 (1990) 920.
[29] N.C. Carpita and D.M. Gibeaut, Plant J. 3 (1993) 1.
[30] N. Lakshminarayanaiah, Transport phenomena in membranes (Academic Press, New York, 1969).
[31] M.D. Walkinshaw and S. Arnott, J. Mol. Biol. 153 (1981) 1075.
[32] P.L. Irwin, M.D. Sevilla and C.L. Stoudt, Biochim. Biophys. Acta 842 (1985) 76.
[33] S. Deiana, G. Micera, G. Muggiolu, C. Gessa and A. Pusino, Colloids Surfaces 6 (1983) 17.
[34] J. Bjerrum, Metal amine formation in aqueous solutions (Haase and son, Copenhagen, 1941).
[35] H.P. Gregor, L.B. Luttinger and E.M. Loebl, J. Phys. Chem. 59 (1955) 34.
[36] P. Van Cutsem and C. Gillet, Plant Physiol. 73 (1983) 865.
[37] J. Dainty and A.B. Hope, Australian J. Biol. Sci. 14 (1961) 541.
[38] Oosawa F., J. Polym. Sci. 23 (1957) 421.
[39] G.S. Manning, J. Chem. Phys. 51 (1969) 924.
[40] G.S. Manning, Quart. Rev. Biophys. 11 (1978) 179.
[41] G.S. Manning and A. Holtzer, J. Phys. Chem. 77 (1973) 2207.
[42] G.S. Manning, J. Phys. Chem. 85 (1981) 870.
[43] F. Oosawa, Polyelectrolytes (Marcel Dekker, New York, 1971).
[44] C. Richter and J. Dainty, Can. J. Bot. 67 (1989) 451.
[45] C. Richter and J. Dainty, Can. J. Bot. 68 (1989) 773.